Kinetic and thermodynamic parameters of copper–dioxygen interaction with different oxygen binding modes

Kenneth D. Karlin [a], William B. Tolman [b], Susan Kaderli [c],
Andreas D. Zuberbühler [c, *]

[a] *Department of Chemistry, The Johns Hopkins University, Baltimore, Maryland 21218, USA*
[b] *Department of Chemistry, University of Minnesota, Minneapolis, MN 55455, USA*
[c] *Institute of Inorganic Chemistry, University of Basel, Spitalstrasse 51, CH-4056 Basel, Switzerland*

Abstract

Kinetic and thermodynamic parameters for metal ion–O_2 interaction have been obtained for a variety of copper(I) complexes with different binding modes for dioxygen. In general, favorable binding enthalpies of up to 80 kJ mol^{-1} are compensated by strongly negative reaction entropies up to -220 J K^{-1} mol^{-1}, restricting the range of overall stabilities. Sequential formation of superoxo and peroxo complexes, as well as concomitant formation of $\eta^1{:}\eta^1$ and $\eta^2{:}\eta^2$ μ-peroxo complexes has been established by low-temperature stopped-flow experiments. In several cases, pseudoreversible binding of dioxygen is followed by an irreversible oxidation of the organic ligand. A recent result is the identification of a rapid equilibrium between an $\eta^2{:}\eta^2$ μ-peroxo complex and the isomeric bis-μ-oxo compound with broken O–O bond which may be fundamental to several O_2 dependent redox enzymes.

Keywords: Dioxygen binding; Activation parameters; Dioxygen carriers; Stoppped-flow kinetics; Copper complexes; Copper protein models

1. Introduction

Four main binding modes I–IV have been established for the interaction of transition metal complexes with dioxygen. As shown in Fig. 1 they can be presented in the form of a 2×2 matrix: End-on binding, as found in hemoglobin, and side-on binding, as in hemocyanin both may be combined with $M^{n+}{:}O_2 = 1{:}1$ (superoxo) and $M^{n+}{:}O_2 = 2{:}1$ (peroxo stoichiometry).

All four geometries have been proposed for Cu^+ as the central atom and three of them have been definitely characterized by X-ray analysis: II [1], III [2], IV [3,4].

In the following our present knowledge on kinetic and thermodynamic parameters of pseudoreversible copper–dioxygen binding will be summarized and discussed in relation to the steric and electronic properties of the corresponding complexes. Where appropriate, the redox activity of the adducts formed will be included. Complexes with five types of ligand will be addressed in turn: (1) Bis-(2-pyri-

* Corresponding author. Tel.: +41-61-2671009; fax: +41-61-2671020; e-mail: zuberbuehle@ubaclu.unibas.ch.
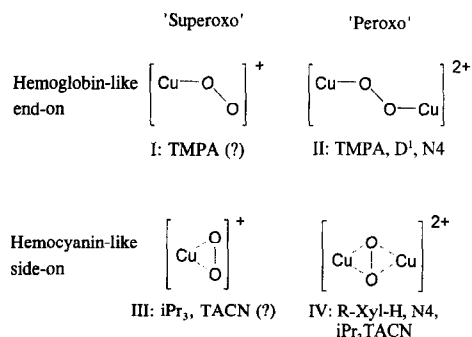
'Superoxo'   'Peroxo'

Hemoglobin-like
end-on $\left[Cu-O_{}O \right]^{+}$ $\left[Cu-O_{}O-Cu \right]^{2+}$

I: TMPA (?)   II: TMPA, D^1, N4

Hemocyanin-like
side-on $\left[Cu_{}^{O}{}_{O} \right]^{+}$ $\left[Cu_{}^{O}{}_{O}Cu \right]^{2+}$

III: iPr_3, TACN (?)   IV: R-Xyl-H, N4,
iPr_3TACN

Fig. 1. Binding modes of dioxygen moiety to copper complexes discussed below.

dylethyl)amine units linked by a m-xylylene spacer (R–Xyl–H and R–Xyl–O$^-$), (2) mononuclear derivatives of tris(2-pyridylmethyl)amine (TMPA), (3) binuclear derivatives of TMPA (D^1), (4) bis-(2-pyridylethyl)amine units linked by an aliphatic carbon chain (N4), and (5) complexes with N-isopropyl substituted 1,4,7-triazacyclononane (iPr_3TACN). Results presented in this contribution all have been obtained by numerical analysis of low-temperature stopped-flow diode array spectrophotometric experiments [5,6].

2. $[Cu_2(R–Xyl–H)]^{2+}$ and $[Cu_2(H–Xyl–O)]^+$ complexes in CH_2Cl_2

The binuclear complex ions $[Cu_2(R–Xyl–H)]^{2+}$, **1a**, and $[Cu_2(H–Xyl–O)]^+$, **1b**, have been the first low-molecular copper species shown to pseudoreversibly bind dioxygen at low temperature in organic solvents [7–9]. As **1a** also clearly and specifically oxygenates the arene spacer in 2-position, it has been proposed as a model for tyrosinase [10]. The kinetic steps of the reaction are represented in Scheme 1. They relate to binding of O_2 (k_1), dissociation of O_2 (k_{-1}) and oxygenation (k_2). Kinetic and thermodynamic parameters for the parent compound, the nitro, $-t$-Bu and fluoro derivatives, as well as for the phenoxo species $[Cu_2(H–Xyl–O)]^+$ (**1b**) are collected in Table 1.
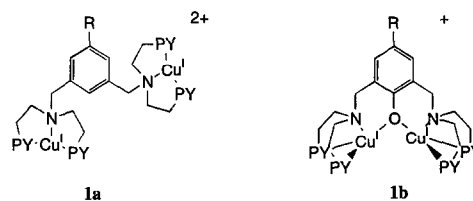
1a   **1b**

Table 1
Kinetic and thermodynamic parameters of $[Cu_2(R–Xyl–H)]^{2+}$ and $[Cu_2(H–Xyl–O)]^+$ complexes

		R				
		NO_2	H	$C(CH_3)_3$	F	H–Xyl–O$^-$
k_1 (M^{-1} s^{-1})	183 K	110	410	470	7.2	—[a]
	223 K	280	1300	1700	270	—[a]
	ΔH^*	6.4 ± 0.1	8.2 ± 0.1	9.1 ± 0.3	29 ± 1	—[a]
	ΔS^*	-167 ± 1	-146 ± 1	-140 ± 1	-66 ± 1	—[a]
k_{-1} (s^{-1})	183 K	$2.1 \cdot 10^{-5}$	$1.6 \cdot 10^{-5}$	$4.3 \cdot 10^{-6}$	$1.5 \cdot 10^{-6}$	—[a]
	223 K	0.027	0.076	0.094	0.025	—[a]
	ΔH^*	59 ± 1	70 ± 1	83 ± 4	81 ± 3	—[a]
	ΔS^*	-8 ± 4	50 ± 6	110 ± 20	90 ± 10	—[a]
k_2 (s^{-1})	183 K	$1.6 \cdot 10^{-5}$	$3.0 \cdot 10^{-4}$	$6.3 \cdot 10^{-3}$	$1.5 \cdot 10^{-3}$	—[b]
	223 K	0.013	0.13	0.96	0.18	—[b]
	ΔH^*	55 ± 1	50 ± 1	41 ± 2	39 ± 1	—[b]
	ΔS^*	-32 ± 2	-35 ± 2	-59 ± 8	-82 ± 6	—[b]
K_1 (M^{-1})	183 K	$6.7 \cdot 10^6$	$2.9 \cdot 10^7$	$1.2 \cdot 10^8$	$5.0 \cdot 10^6$	$6.5 \cdot 10^8$
	223 K	$1.3 \cdot 10^4$	$1.9 \cdot 10^4$	$1.9 \cdot 10^4$	$1.1 \cdot 10^4$	$2.7 \cdot 10^5$
	$\Delta_r H^{\ominus}$	-53 ± 1	-62 ± 1	-74 ± 4	-52 ± 3	-66 ± 1
	$\Delta_r S^{\ominus}$	-159 ± 4	-196 ± 6	-250 ± 20	-156 ± 10	-192 ± 2

[a] Equilibration with O_2 in less than 5 ms at $-95°C$.
[b] No oxygenation possible.
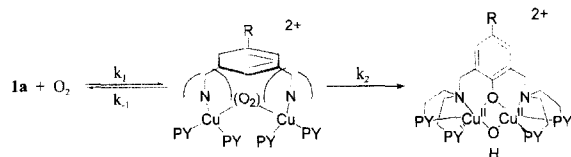
Scheme 1. Oxygen binding to $[Cu_2(R-Xyl-H)]^{2+}$ followed by oxygenation.

As can be seen, binding of O_2 to these binuclear complexes is characterized by very low activation enthalpies of less than 10 kJ mol^{-1}, which are compensated by strongly unfavorable activation entropies of -140 to -170 J K^{-1} mol^{-1}. The somewhat larger activation enthalpy of 29 kJ mol^{-1} for the fluoro compound is explained by freezing out of a complex conformation which is unfit for oxygen binding at low temperatures [9].

With respect to enthalpy, binding of O_2 (K_1) is increased, dissociation (k_{-1}) disfavored, and the rate of oxygenation (k_2) increased by the electron donating t-Bu group, while the opposite trend is observed for the nitro compound. In each case favorable enthalpy is again at least partially compensated by a disfavorable (more negative) entropy term.

With this series of xylyl spaced binuclear copper complexes it has been shown that low temperature and organic solvents may help to stabilize copper–dioxygen adducts.

Dioxygen binding may be as strong as in biological dioxygen carriers, but room temperature stability is precluded by unfavorable entropies in these low-molecular systems. The trend in the kinetic parameters along with additional observations such as the absence of an isotope effect in the oxygenation step conveys the characteristics of a strong electrophile.
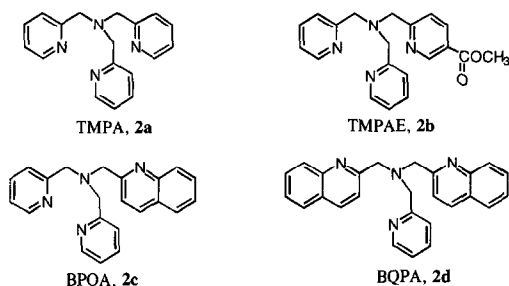
Table 2
Kinetic parameters of $[Cu(TMPA)]^+$ and its derivatives

		$[Cu(TMPA)]^+$	$[Cu(TMPAE)]^+$	$[Cu(BPQA)]^+$	$[Cu(BQPA)]^+$
k_1 (M^{-1} s^{-1})	183 K	$2 \cdot 10^4$	$8.2 \cdot 10^3$	— [a]	18
	298 K	$8 \cdot 10^7$	$4 \cdot 10^7$	— [a]	$6 \cdot 10^4$
	ΔH^*	32 ± 4	31 ± 5	— [a]	30 ± 2
	ΔS^*	14 ± 18	5 ± 29	— [a]	-53 ± 8
k_{-1} (s^{-1})	183 K	8	29	— [a]	$6 \cdot 10^{-3}$
	298 K	$2 \cdot 10^8$	$4 \cdot 10^8$	— [a]	$2 \cdot 10^5$
	ΔH^*	66 ± 4	63 ± 5	— [a]	65 ± 4
	ΔS^*	137 ± 18	132 ± 29	— [a]	72 ± 19
k_2 (M^{-1} s^{-1})	183 K	$3 \cdot 10^4$	$1.52 \cdot 10^4$	— [a]	— [b]
	298 K	$1.8 \cdot 10^6$	$5.8 \cdot 10^6$	— [a]	— [b]
	ΔH^*	14 ± 1	21 ± 1	— [a]	— [b]
	ΔS^*	-78 ± 2	-43 ± 3	— [a]	— [b]
k_{-2} (s^{-1})	183 K	$1.5 \cdot 10^{-4}$	$2.1 \cdot 10^{-5}$	$1.9 \cdot 10^{-4}$	— [b]
	298 K	$1.2 \cdot 10^3$	$7 \cdot 10^2$	$1.6 \cdot 10^3$	— [b]
	ΔH^*	61 ± 3	66 ± 1	61 ± 1	— [b]
	ΔS^*	19 ± 10	33 ± 5	21 ± 4	— [b]
k_{on} (M^{-2} s^{-1})	183 K	$6 \cdot 10^7$	$4.3 \cdot 10^6$	$3 \cdot 10^6$	— [b]
	298 K	$6 \cdot 10^5$	$5.2 \cdot 10^5$	$7 \cdot 10^5$	— [b]
	ΔH^*	-20 ± 2	-10.3 ± 0.2	-8 ± 1	— [b]
	ΔS^*	-201 ± 5	-170 ± 1	-160 ± 2	— [b]

[a] Superoxo complex not observed with $[Cu(BPQA)]^+$.
[b] Only thermodynamic parameters obtained.

3. Mononuclear copper complexes with TMPA and some derivatives in EtCN

TMPA, 2a   TMPAE, 2b

BPQA, 2c   BQPA, 2d

Scheme 2. Consecutive formation of superoxo and peroxo adducts with complexes of 2a–2d.

The complex with tris(2-pyridylmethyl)amine (TMPA, 2a) has been the first for which a copper peroxo complex $[\{Cu(TMPA)\}_2O_2]^{2+}$ has been isolated and characterized by X-ray crystallography [1]. It pseudoreversibly binds dioxygen as is equally observed with the complexes derived from the analogous ligands TMPAE (2b), BPQA (2c) and BQPA (2d). Also for the first time, in these systems the consecutive formation of superoxo and peroxo complexes could be followed as indicated in Scheme 2 [5,11].

Kinetic as well as thermodynamic parameters for TMPA and its derivatives TMPAE, BPQA, and BQPA are collected in Tables 2 and 3.

The results may be summarized as follows:

Activation enthalpies for initial dioxygen binding (k_1) as well as for Cu–O bond splitting (k_{-1}, k_{-2}) are essentially identical for the different complexes. Activation enthalpies of roughly 65 kJ mol^{-1} equally pertain to Cu–O bond splitting in superoxo (k_{-1}) and in peroxo species (k_{-2}). Low rate constants with the sterically hindered BQPA are exclusively due to unfavorable entropies relative to TMPA and TMPAE. Activation enthalpies around 30 kJ mol^{-1} for formation of the first copper–oxygen bond (k_1) are substantial and considerably higher than those found for $[Cu_2(R\text{-}Xyl\text{-}H)]^{2+}$. On the other hand, negative activation enthalpies, i.e. decreasing rate with increasing temperature are observed for the overall peroxo formation $k_{on} = k_1 k_2 / k_{-1}$. Binding constants for superoxo complexes (K_1) and the corresponding thermodynamic parameters are virtually identical, but

Table 3
Thermodynamic parameters of $[Cu(TMPA)^+$ and its derivatives

|		$[Cu(TMPA)]^+$	$[Cu(TMPAE)]^+$	$[Cu(BPQA)]^+$	$[Cu(BQPA)]^+$
K_1 (M^{-1})	183 K	$1.9 \cdot 10^3$	$2.8 \cdot 10^2$	—[a]	$2.9 \cdot 10^3$
	298 K	0.34	$9 \cdot 10^{-2}$	—[a]	0.4
	$\Delta_r H^\ominus$	-34 ± 1	-32 ± 1	—[a]	-35 ± 6
	$\Delta_r S^\ominus$	-123 ± 4	-127 ± 3	—[a]	-125 ± 27
K_2 (M^{-1})	183 K	$2.2 \cdot 10^8$	$7 \cdot 10^8$	—[a]	$2.0 \cdot 10^3$
	298 K	$1.5 \cdot 10^3$	$8 \cdot 10^3$	—[a]	40
	$\Delta_r H^\ominus$	-47 ± 3	-45 ± 1	—[a]	-15
	$\Delta_r S^\ominus$	-97 ± 10	-76 ± 6	—[a]	-20
$\beta_2 = K_1 K_2$	183 K	$4.3 \cdot 10^{11}$	$2.1 \cdot 10^{11}$	$1.7 \cdot 10^{10}$	$6 \cdot 10^6$
	298 K	$5 \cdot 10^2$	$7 \cdot 10^2$	$4.4 \cdot 10^2$	20
	$\Delta_r H^\ominus$	-81 ± 3	-77 ± 1	-69 ± 2	-50
	$\Delta_r S^\ominus$	-220 ± 11	-203 ± 5	-181 ± 5	-145

[a] Not observed.

steric hindrance leads to destabilization of peroxo complexes with BPQA and BQPA (K_2, β_2). Based on the inspection of space filling models and in line with the structure of the corresponding peroxo complex [1], end-on coordination of O_2 (Fig. 1, I) is suggested for the superoxo complex $[(TMPA)Cu(O_2)]^+$.

With this series of mononuclear tripodal ligands consecutive formation of superoxo copper complexes followed by binuclear peroxo species has been observed for the first time. As with $[Cu_2(R-Xyl-H)]^{2+}$, room temperature stability is precluded by strongly negative reaction entropies.

4. Binucleating derivative of TMPA: $[Cu_2(D^1)]^{2+}$

The binuclear complex ion $[Cu_2(D^1)(EtCN)]^{2+}$, 3 has been studied in the hope that linking two TMPA moieties would overcome a significant part of the unfavorable reaction entropies of -220 to -203 J K^{-1} mol^{-1} observed with TMPA and TMPAE for peroxo formation (β_2, Table 3) by a sort of inverse chelate effect (Scheme 3).

Because of the nature of the complex with independently reacting metal centers and the bidentate properties of O_2, a complicated kinetic scheme including an open and a closed form of $[Cu_2(D^1)(O_2)]^{2+}$, bis superoxo $[Cu_2(D^1)(O_2)_2]^{2+}$ and an annular trimeric species $[\{Cu_2(D^1)(O_2)\}_3]^{6+}$ have been established [6,12]. Here, we restrict ourselves to the
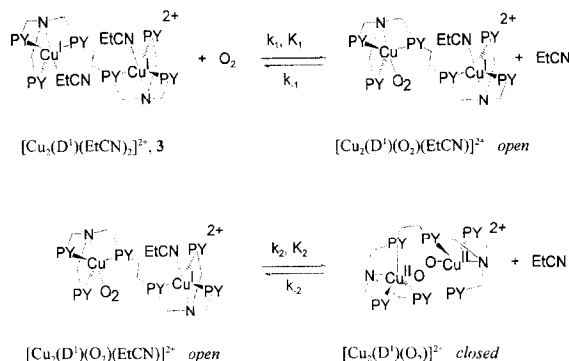
Scheme 3. Kinetic steps leading to intramolecular peroxo formation with $[Cu_2(D^1)(EtCN)_2]^{2+}$.

comparison of intramolecular peroxo formation with D^1 in relation to the corresponding intermolecular process with TMPA. The relevant parameters are collected in Table 4.

As evidenced very clearly by the data collected in Table 4, the binucleating nature of D^1 indeed leads to significant entropic stabilization of the intramolecular peroxo complex in relation to $[\{(TMPA)Cu\}_2O_2]^{2+}$. Activation entropies for O_2 binding (k_2, k_{on}) are more favorable by 60–70 J K^{-1} mol^{-1} for 3, in addition copper–dioxygen bond splitting (k_{-2}) is entropically *dis*favored for the binuclear complex, again by 70 J K^{-1} mol^{-1}. In consequence, we have a very substantial entropic stabilization by 130–140 J K^{-1} mol^{-1} for K_2 and β_2 for the closed (peroxo) form of $[Cu_2(D^1)(O_2)]^{2+}$ in relation to $[\{(TMPA)Cu\}_2O_2]^{2+}$. The practically identical values of K_1 for the superoxo complexes with D^1 and TMPA containing a single copper–dioxygen bond, strongly supports the explanation

Table 4
Kinetics and thermodynamic parameters for peroxo formation with $[Cu_2(D^1)(EtCN)_2]^{2+}$ in EtCN

	TMPA		D^1	
	ΔH^* (kJ mol^{-1})	ΔS^* (J K^{-1} mol^{-1})	ΔH^* (kJ mol^{-1})	ΔS^* (J K^{-1} mol^{-1})
k_2	14 ± 1	-78 ± 2	37 ± 1	-9 ± 3
k_{-2}	61 ± 3	19 ± 10	37 ± 1	-49 ± 3
$k_{on} = k_1 k_2 / k_{-2}$	-20 ± 2	-201 ± 5	1.7 ± 0.6	-139 ± 3
K_1	-34 ± 1	-123 ± 4	-35 ± 1	-129 ± 2
K_2	-47 ± 3	-97 ± 10	0.5 ± 0.6	40 ± 3
$\beta_2 = K_1 K_2$	-81 ± 3	-220 ± 11	-35 ± 1	-89 ± 2

of entropic stabilization by the proposed inverse chelate effect with D^1. Unfortunately, favorable entropy terms with **3** are essentially offset by concomitant enthalpic destabilization, again noticed for kinetic as well as for thermodynamic parameters. Activation enthalpies for D^1 are 20 kJ mol^{-1} *higher* for dioxygen binding (k_2, k_{on}), but more than 20 kJ mol^{-1} *lower* for Cu–O bond splitting (k_{-2}) as compared to TMPA. As a consequence, the overall reaction enthalpy for D^1 is reduced to -35 kJ mol^{-1} from -81 kJ mol^{-1} for TMPA and in fact, ring closure (peroxo formation) itself (K_2) has a negligible reaction enthalpy or is even slightly endothermic (0.5 kJ mol^{-1}).

Complexes derived from binucleating ligands may indeed entropically favor formation of intramolecular peroxo adducts, but with D^1 this is offset by enthalpic destabilization. In fact, intramolecular strain in $[Cu_2(D^1)(O_2)]^{2+}$ is released by oligomerization.

## 5. Bis-(2-pyridylethyl)amine units linked by an aliphatic C_4 chain: $[Cu_2(N4)]^{2+}$ in CH_2Cl_2

The binuclear complex $[Cu_2(N4)]^{2+}$ (**4**) has a coordination sphere which is essentially identical to that of the $[Cu_2(R–Xyl–H)]^{2+}$ (**1a**) complexes discussed above. With the more flexible aliphatic $-(CH_2)_4-$ linking unit and the absence of an obvious position for electrophilic substitu-
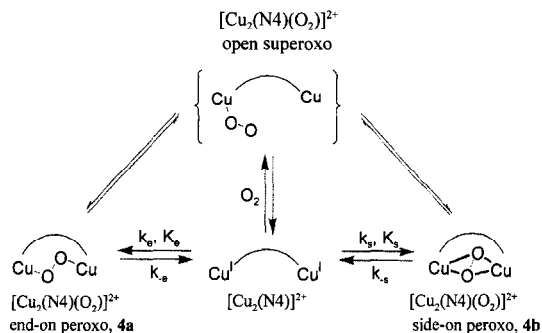
Scheme 4. Interconversion of annular end-on and side-on peroxo complexes $[Cu_2(N4)(O_2)]^{2+}$ through the intermediacy of an open-chain superoxo complex.

tion, **4** might be expected to react faster than **1a** with O_2 and to form a more stable adduct. In addition, a very simple kinetic situation with pseudoreversible dioxygen binding and release might be anticipated. While the former two expectations where fulfilled, dioxygen binding kinetics were in fact more complicated with concomitant formation of two different peroxo complexes and subsequent equilibration through an open-chain superoxo species [13], as shown in Scheme 4.
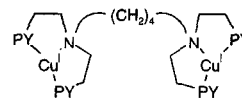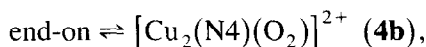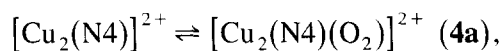

4, PY=2-pyridyl

Table 5
Kinetic, thermodynamic and spectral parameters of $[Cu_2(N4)]^{2+}$

		$[Cu_2(N4)(O_2)]^{2+}$		$[Cu_2(H–Xyl–H)(O_2)]^{2+}$
		end-on	side-on	side-on
k (M^{-1} s^{-1})	183 K	$1.1 \cdot 10^4$	$8.5 \cdot 10^3$	$4.1 \cdot 10^2$
	223 K	$1.4 \cdot 10^4$	$8 \cdot 10^4$	$1.3 \cdot 10^3$
	ΔH^*	0 ± 3	18 ± 2	8.2 ± 0.1
	ΔS^*	-162 ± 18	-70 ± 9	-146 ± 1
K (M^{-1})	183 K	$4.5 \cdot 10^2$	$7 \cdot 10^7$	$2.9 \cdot 10^7$
	223 K	$1.8 \cdot 10^1$	$8 \cdot 10^5$	$1.9 \cdot 10^4$
	$\Delta_r H^\ominus$	-28 ± 3	-58 ± 2	-62 ± 1
	$\Delta_r S^\ominus$	-101 ± 19	-165 ± 8	-196 ± 6
λ_{max}		525 nm	456 nm	440 nm

In line with observations for **1a** and with the mononuclear complex of bis-(2-pyridylethyl)methylamine the superoxo species merely exists as a steady-state species and is invoked to avoid the necessity of synchronous binding of two copper ions to O_2 upon formation of the peroxo complexes. Direct sequential formation of the end-on and side-on species on the other hand is precluded by the details of kinetic analysis,

$$[Cu_2(N4)]^{2+} \rightleftharpoons [Cu_2(N4)(O_2)]^{2+} \quad \textbf{(4a)},$$

$$\text{end-on} \rightleftharpoons [Cu_2(N4)(O_2)]^{2+} \quad \textbf{(4b)},$$

side-on.

Based on spectroscopic evidence [13,14], the thermodynamically favored product is assigned an $\eta^2:\eta^2$ side-on μ-peroxo coordination related to the one of $[Cu_2(H-Xyl-H)(O_2)]^{2+}$ as borne out by similar λ_{max} of 456 and 440 nm, respectively. Also, the thermodynamic parameters are closely related to those of $[Cu_2(H-Xyl-H)(O_2)]^{2+}$ with $\Delta_r H^{\ominus} = -58 \pm 2$ versus -62 ± 1 kJ mol^{-1} and $\Delta_r S^{\ominus} = -165 \pm 8$ versus 196 ± 6 J K^{-1} mol^{-1} (Table 5).

Again based on spectral characteristics ($\lambda_{max} = 525$ nm, shoulder near 600 nm) the thermodynamically less stable of the two species is assigned an $\eta^1:\eta^1$ μ-peroxo coordination related to the one established for $[\{Cu(TMPA)\}_2(O_2)]^{2+}$ by X-ray analysis [1]. At 183 K, **4a** is formed somewhat more quickly ($k = 1.1 \cdot 10^4$ M^{-1} s^{-1}) than **4b** ($k = 8.5 \cdot 10^3$ M^{-1} s^{-1}), both significantly faster than $[Cu_2(H-Xyl-H)(O_2)]^{2+}$ ($k = 4.1 \cdot 10^2$ M^{-1} s^{-1}). The activation enthalpy is zero within experimental error and the reaction enthalpy of **4a** is only half that of **4b**, -28 versus -58 J K^{-1} mol^{-1}. Despite a slightly more favorable reaction entropy this leads to a significantly reduced binding constant of $4.5 \cdot 10^2$ M^{-1} for **4a** against $7 \cdot 10^7$ M^{-1} for **4b** at 183 K.

Increased flexibility in binuclear complexes may increase the rate of dioxygen binding. End-on $\eta^1:\eta^1$ and side-on $\eta^2:\eta^2$ μ-peroxo complex formation have been observed for the first time in the same system. In the absence of steric hindrance, the latter seems to be thermodynamically more favorable. Conformational changes induced by the transition of end-on to side-on complexation might be responsible for the induction of cooperative effects in hemocyanin.

6. Complexes with *N*-isopropyl substituted 1,4,7-triazacyclononane: $[Cu(iPr_3TACN)]^+$

5
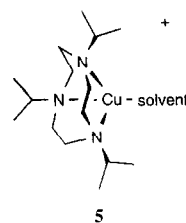
$[Cu(iPr_3TACN)]^+$, **5**, has been shown to form an $\eta^2:\eta^2$ μ-peroxo complex [15] closely related to that first described by Kitajima for trispyrazolyl borate complexes [3] and later for oxyhemocyanin [16]. At low temperature the kinetics of adduct formation in acetone are given by a simple second order rate law (1) [17], this is supplemented by oxidative cleavage of an isopropyl group above $-50°C$ [15],

$$-d[O_2]/dt = k[\{Cu(iPr_3TACN)\}^+][O_2] \quad (1)$$
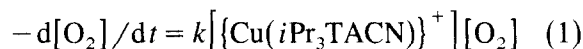
Activation parameters closely match those obtained for superoxo adduct formation with $[Cu(BQPA)]^+$: $\Delta H^{\neq} = 37.2 \pm 0.5$ and 30 ± 2 kJ mol^{-1}; $\Delta S^{\neq} = -62 \pm 2$ and -53 ± 8 J K^{-1} mol^{-1}, respectively. They are quite in contrast to the values observed for peroxo formation with $[Cu_2(H-Xyl-H)]^+$ and TMPA, characterized by low or even negative activation enthalpies and very unfavorable activation entropies. The experimental rate law, the absence of any observable intermediates, and the values for the activation parameters all point to superoxo complex formation in the rate limiting step. Without experimental evidence at hand, the corresponding steady state species is assumed to have the same side-on binding mode as obtained with a highly substituted pyrazolylborate [2].
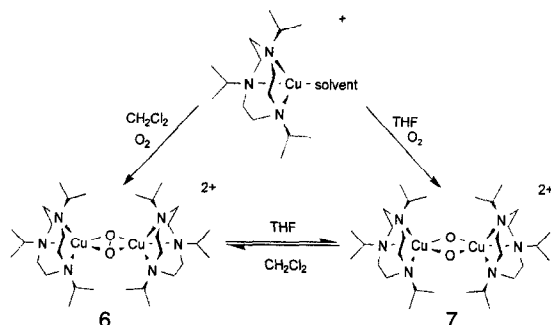
Scheme 5. Interconversion of $\eta^2{:}\eta^2$ μ-peroxo and bis μ-oxo copper complexes with iPr$_3$TACN.

While the kinetics of [Cu(iPr$_3$TACN)]$^+$/O$_2$ interaction are unspectacular, the corresponding adduct possesses exciting new and so far unique properties. In acetone the peroxo complex [{Cu(iPr$_3$TACN)$_2$}(O$_2$)]$^{2+}$ (6) forms absolutely in parallel with an isomeric bis-μ-oxo species [{Cu(iPr$_3$TACN)$_2$}(O)$_2$]$^{2+}$ (7). A structure analogous to 7 has been characterized by X-ray crystallography with benzyl substituted TACN [17]. Rapid interconversion of 6 and 7 (Scheme 5) has been demonstrated by the addition of CH$_2$Cl$_2$ or THF which specifically stabilizes structures 6 and 7, respectively. The relevance of this observation should be obvious:

Rapid interconversion of [M$_2$(μ-$\eta^2{:}\eta^2$-O$_2$)]$^{2+}$ (peroxo) and [M$_2$(μ-O)$_2$]$^{2+}$ (oxo/oxyl) complexes has been observed for the first time. It may be a key step both in dioxygen evolution during photosynthesis and in dioxygen reduction by various enzymes such as cytochrome-C-oxidase or tyrosinase.

7. Conclusion

Kinetic and thermodynamic parameters for metal ion/O$_2$ interaction have been obtained for a variety of copper(I) complexes with different binding modes for dioxygen. In the systems studied so far we have observed a general trend of compensating favorable enthalpies with less favorable entropies and vice versa, restricting the range of overall stabilities.

Sequential formation of superoxo and peroxo complexes, as well as concomitant formation of $\eta^1{:}\eta^1$ and $\eta^2{:}\eta^2$ μ-peroxo complexes has been established by low-temperature stopped-flow experiments. A recent result of these studies is the identification of a rapid equilibrium between an $\eta^2{:}\eta^2$ μ-peroxo complex and the isomeric bis-μ-oxo compound with broken O–O bond which may be fundamental to several O$_2$ dependent redox enzymes.

References

[1] Z. Tyeklár, R.R. Jacobson, N. Wei, N.N. Murthy, J. Zubieta and K.D. Karlin, J. Am. Chem. Soc. 115 (1993) 2677.
[2] K. Fujisawa, M. Tanaka, Y. Moro-oka and N. Kitajima, J. Am. Chem. Soc. 116 (1994) 12079.
[3] N. Kitajima, K. Fujisawa, Y. Moro-oka and K. Toriumi, J. Am. Chem. Soc. 111 (1989) 8975.
[4] N. Kitajima, K. Fujisawa, C. Fujimoto, Y. Moro-oka, S. Hashimoto, T. Kitagawa, K. Toriumi, K. Tatsumi and A. Nakamura, J. Am. Chem. Soc. 114 (1992) 1277.
[5] K.D. Karlin, N. Wei, B. Jung, S. Kaderli, P. Niklaus and A.D. Zuberbühler, J. Am. Chem. Soc. 115 (1993) 9506.
[6] D.-H. Lee, N. Wei, N.N. Murthy, Z. Tyeklár, K.D. Karlin, S. Kaderli, B. Jung and A.D. Zuberbühler, J. Am. Chem. Soc. 117 (1995) 12498.
[7] K.D. Karlin, R.W. Cruse, Y. Gultneh, A. Farooq, J.C. Hayes and J. Zubieta, J. Am. Chem. Soc. 109 (1987) 2668.
[8] R.W. Cruse, S. Kaderli, K.D. Karlin and A.D. Zuberbühler, J. Am. Chem. Soc. 110 (1988) 6882.
[9] K.D. Karlin, M.S. Nasir, B.I. Cohen, R.W. Cruse, S. Kaderli and A.D. Zuberbühler, J. Am. Chem. Soc. 116 (1994) 1324.
[10] K.D. Karlin, Y. Gultneh, J.C. Hayes, R.W. Cruse, J. McKnown, J.P. Hutchinson and J. Zubieta, J. Am. Chem. Soc. 106 (1984) 2121.
[11] K.D. Karlin, N. Wei, B. Jung, S. Kaderli and A.D. Zuberbühler, J. Am. Chem. Soc. 113 (1991) 5868.
[12] N. Wei, D.-H. Lee, N.N. Murthy, Z. Tyeklár, K.D. Karlin, S. Kaderli, B. Jung and A.D. Zuberbühler, Inorg. Chem. 33 (1994) 4625.
[13] B. Jung, K.D. Karlin and A.D. Zuberbühler, J. Am. Chem. Soc. 118 (1996) 3763.
[14] N.J. Blackburn, R.W. Strange, A. Farooq, M.S. Haka and K.D. Karlin, J. Am. Chem. Soc. 110 (1988) 4263.
[15] S. Mahapatra, J.A. Halfen, E.C. Wilkinson, L. Que Jr. and W.B. Tolman, J. Am. Chem. Soc. 116 (1994), 9785.
[16] K.A. Magnus, B. Hazes, H. Ton-That, C. Bonaventura, J. Bonaventura and W.G. Hol, Proteins Struct. Funct. Genet. 19 (1994) 302.
[17] J.A. Halfen, S. Mahapatra, E.C. Wilkinson, S. Kaderli, V.G. Young Jr., L. Que Jr., A.D. Zuberbühler and W.B. Tolman, Science 271 (1996) 1397.